NEUTRALIZED DRIFT COMPRESSION EXPERIMENTS (NDCX)

P. K. Roy[1], W. L. Waldron[1], S. S. Yu[1], P. A. Seidl[1], E. Henestroza[1], A. Anders[1], D. Baca[1], J. Barnard[4], F. M. Bieniosek[1], R. J. Briggs[2], C. Celata[1], J. Coleman[1], R. C. Davidson[3], P. C. Efthimion[3], S. Eylon[1], A. Friedman[4], E. P. Gilson[3], W. G. Greenway[1], D. P. Grote[4], I. Kaganovich[3], M. Leitner[1], B. G. Logan[1], H. Qin[3], L. L. Reginato[1], A. B. Sefkow[3], W. M. Sharp[4], C. Thoma[5], and D. R. Welch[5]

[1]*Lawrence Berkeley National Laboratory, 1 Cyclotron Rd, Berkeley, CA94720, USA*
[2]*SAIC, Alamo, CA 94507, USA*
[3]*Princeton Plasma Physics Laboratory, Princeton, New Jersey 08543-0451, USA*
[4]*Lawrence Livermore National Laboratory, Livermore, CA 94550, USA*
[5]*Voss Scientific, Albuquerque, NM 87108, USA*

Abstract

Intense ion beams offer an attractive approach to heating dense matter uniformly to extreme conditions, because their energy deposition is nearly classical and volumetric. Simultaneous transverse and longitudinal beam compression in a neutralizing plasma medium, along with rapid beam acceleration, are being studied as a means of generating such beams for warm dense matter (WDM) and high energy density physics (HEDP) experiments, as well as for inertial fusion. Recent experiments on transverse and longitudinal compression demonstrated significant enhancements in beam intensity. In parallel with the beam compression studies, a new accelerator concept, the Pulse Line Ion Accelerator (PLIA), potentially offers cost-effective high-gradient ion beam acceleration at high line charge density. We describe experimental results on beam neutralization, and neutralized drift compression from a series of experiments. We also describe first the beam dynamics validation experiments exploring the PLIA.

INTRODUCTION

High energy density physics and ion-driven inertial fusion require the simultaneous transverse and longitudinal compression of an ion beam to achieve high intensities with a 1-2mm radius spot size and pulse length of a few nanoseconds. These beams are achievable with beam neutralization via plasma for transverse compression, and beam velocity tailoring via an induction module for longitudinal compression. In beam neutralization, electrons from a background plasma or external source are entrained by the beam and neutralize the space charge sufficiently such that the pulse focuses on the target in a nearly ballistic manner to a small spot size [1-9], limited only by the longitudinal and transverse emittance. In longitudinal compression, the beam is compressed by imposing a linear head-to-tail velocity tilt, which produces a pulse duration of a few ns. The physics on drift compression are well described elsewhere [10-13]. One essential point is that (in the absence of neutralization) longitudinal space-charge forces limit the beam compression ratio, the ratio of the initial to final current, to about ten in most applications. An experiment with five-fold compression has been reported [14]. We report here the achievement of much higher compression ratios in experiments [15] with a high perveance heavy ion beam in a plasma-filled drift region, in which the space-charge forces of the ion beam are neutralized. However, these experiments [15] have to date not attempted simultaneous transverse and longitudinal compression, which is our next goal.

In parallel with the beam compression studies, a new method of accelerating intense ion bunches has been conceived [16-17] and studied using analytic theory and simulations [17-19]. This Pulse Line Ion Accelerator (PLIA) can accelerate beams of any pulse length, in principle, but is best suited as an accelerator for intense bunches with pulse lengths of tens of centimeters. This parameter regime is not well matched to RF accelerators. The major advantage of the PLIA concept is its potential for a significant reduction in the cost per MeV compared to induction linacs, for example. Here we present initial experimental results [20, 21] of the PLIA as a proof-of-principle. However, the acceleration gradient is limited due to vacuum surface flashover, and further study is in progress.

Experimental progress on beam compression and the PLIA is presented below.

BEAM COMPRESSION

Transverse Beam Compression

A K^+ beam was extracted from a variable perveance injector and transported through a 2.4 m long quadrupole lattice for final focusing. Neutralization was provided by a localized cathode arc plasma plug and an RF volumetric plasma system. We experimentally demonstrated [9] that without neutralization, the 24 mA beam radius at the nominal 1-m focal distance was 14.7 mm. When the beam was neutralized by passing it through the 5-cm long arc plasma (referred to as plasma plug) and pulsed RF volumetric plasma source, the beam radius decreased to ~1.3 mm. We also demonstrated that the neutralized beam size depends on convergence angle, beam energy, axial position, but not significantly on the perveance. Finally, it was shown that the parametric variation of the experimental neutralized beam radius was

qualitatively matched with theoretical predictions. An example of such a neutralized focusing result is shown in Fig. 1. Experimental details to provide active neutralization are presented elsewhere [4-9].

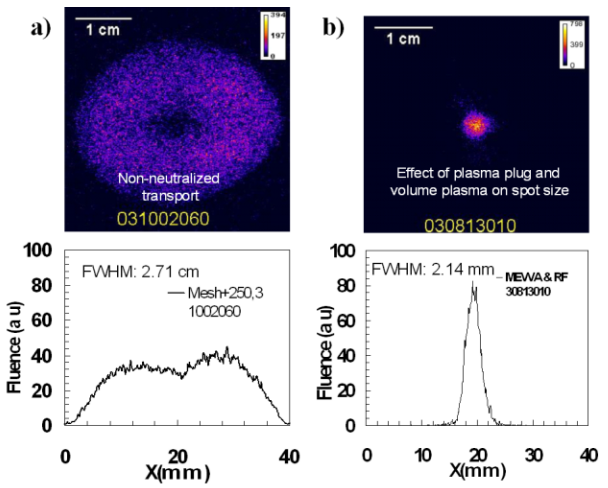

Figure1: Experimentally measured beams as focused (a) non-neutralized (signals reduced at the center of the image due to scintillator degradation); (b) neutralized.

Longitudinal Beam Compression

The NDCX experiment used the same front end as the earlier Neutralized Transport experiment (NTX) [4-9]. To provide the head-to-tail velocity tilt, an induction module with a variable voltage waveform was placed immediately downstream of the last quadrupole magnet. The plasma column was formed by two pulsed aluminum cathodic arc source located at the downstream end. During the experiment [15], it was observed that the position of maximal compression varied with the beam energy for a given voltage waveform.

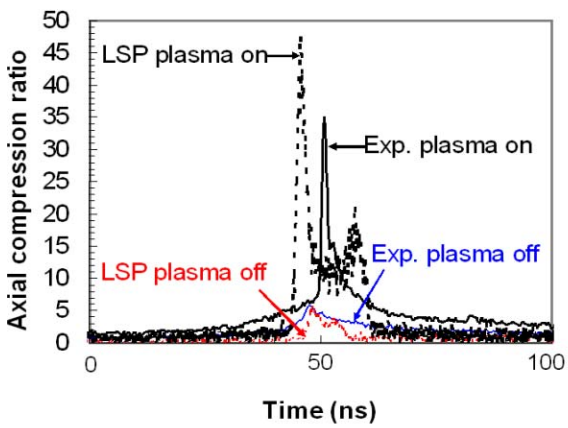

Figure 2: Experimental data and LSP simulation of beam compression with neutralization (plasma source on), and without neutralization (plasma source off).

The strong effects of neutralization are evident by comparing the compression ratio when the plasma turned on and off. Figure 2 shows significantly reduced peak current when the plasma is turned off. The particle-in-cell code LSP shows qualitatively similar results. Note that the simulated beam energy and observing station do not exactly matched those of the experiment, which was responsible for the different peak locations between the simulations and the experiment.

The maximum compression is observed by fine tuning the beam energy to match the voltage waveform and precisely position the longitudinal focal point at the diagnostic location as shown in Fig. 3. The compression ratio of about 50, seen in Fig. 3(b), is obtained by taking the ratio of the signal with velocity tilt on (with compression) to the signal with tilt voltage off (without compression); see Fig. 3(a). A similar result is measured with the fast 'pinhole' Faraday cup [22]; see Fig. 3(c). LSP simulations under these experimental conditions predict a peak compression ratio of 60 [Fig.3 (d)].

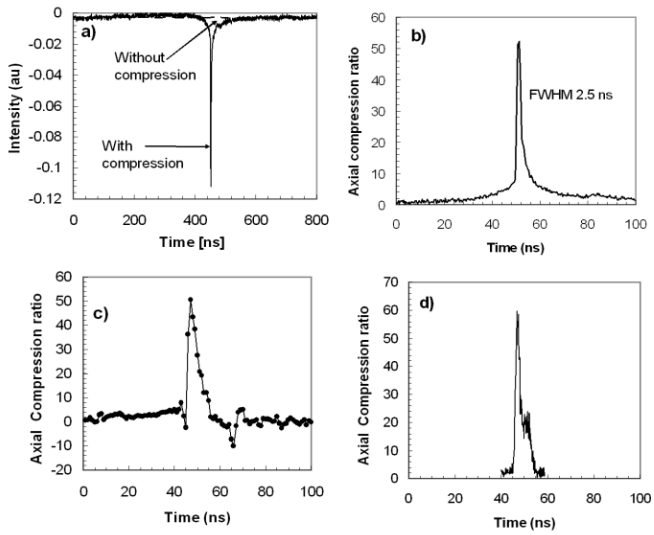

Figure 3: (a) Measurements of beam signal using the phototube diagnostic for neutralized non-compressed, and neutralized compressed beams; (b) compression ratio obtained from the measurements using the phototube; (c) compression ratio obtained from measurements using the Faraday cup; and (d) LSP simulation for axial compression ratio under the experimental conditions.

The transverse beam size as a function of time during longitudinal compression has also been measured. The measured spots for the 1-m beam focusing angle had roughly a 6-mm radius [15]. It is interesting to observe that the transverse spot size is larger at the point of maximum compression. This feature is due to time-dependent defocusing effects occurring at the induction gap, and is also seen in LSP simulations. We have performed additional experiments with the plasma-filled drift length extended to two meters. We are able to recover the 50-fold compression in the 2-m experiment. On the basis of this two-meter experiment we conclude that: 1) the degree of charge neutralization is sufficient to achieve 50-fold longitudinal compression while avoiding space-charge blow-up of the beam for the experimental configuration investigated; 2) the intrinsic longitudinal

temperature is less than 1eV; and 3) no collective instabilities are observed.

Simultaneous Transverse and Longitudinal Beam Compression

To obtain higher compression ratio, the required induction module waveform must be extended in time keeping a constant-slope velocity ramp imparted to the beam. Thus, a larger segment of the beam will be compressed. If the beam longitudinal temperature is fixed, more beam charge can then be compressed at a given plane yielding a larger compression ratio. The larger beam energy spread, however, can complicate the transverse focusing at this plane. Simultaneous transverse and longitudinal compression with several approaches have been made on the basis of current simulations [8, 23-25].

Simulations [25] indicate that a 400 keV K^+ ion beam can be transversely and longitudinally compressed in current density by a factor greater than 10^5 over a distance of 2.5 m. Such an intense pulse can be achieved as long as various system components are optimized; a controlled voltage waveform can impart a nearly-ideal axial velocity tilt to the ion beam, which can be transversely focused to the longitudinal focal plane by a strong final-focus solenoid. The transverse and longitudinal beam temperatures contribute to focusing aberrations in both directions, and are limiting factors for achieving small spot sizes and short pulse durations. In near-term experiments on the simultaneous transverse and longitudinal compression experiment, the solenoidal plasma channel is replaced by a ferroelectric plasma source. This new plasma source provides plasma from discharges on the inner surface of a ceramic-lined drift column [26]. Along with the new plasma column, the induction module voltage waveform is to be optimized by changing its duration and amplitude.

PULSE LINE ION ACCELERATOR

As mentioned in the Introduction, the pulse line ion accelerator (PLIA) [17] is a new beam acceleration technique. The PLIA is a helical coil structure, submerged in a dielectric medium and powered by a pulsed high-voltage waveform to impart beam energy gains many times higher than the input voltage. Figure 4(a) is a schematic representation of a helical pulse line structure which creates a voltage waveform as shown in Fig. 4 (b). Figure 4(c) shows the helical structure for this experiment. A primary strap with one or two turns, driven by a low-impedance pulsed-power source is placed a short distance radially outward from the grounded input end of the helix. A fraction of the flux created by the primary strap links to the helix, and this flux generates an axial voltage gradient along the input region of the helix. Downstream, the helix is terminated into its characteristic impedance via a string of resistors helically wound with a pitch similar to that of the helix. This serves to minimize reflections which could distort the voltage waveform. A pulsed drive on the primary strap creates a voltage on the helix that builds up over the primary coupling region.

Figure 5 shows a sketch of the PLIA setup with a 350 keV K^+ ion beam line. Four pulsed quadrupole magnets are used to control the beam envelope. The beam is apertured to ~1mA upstream of the PLIA section. Two removable diagnostics, separated by 1m, are located downstream of the helix section to measure the beam current profile, followed by an electrostatic energy analyzer (EEA) to measure the longitudinal phase space. Before powering the helix section, the head-to-tail energy profile of the 350 keV, long-pulse (19 μs) beam is measured using the EEA. Except for beam dynamics effects introduced by time-of-flight and beam aperturing, the Marx waveform and the EEA energy profile are similar. The energy distribution provided by the EEA agrees with the capacitive monitor of the Marx voltage to about 2%.

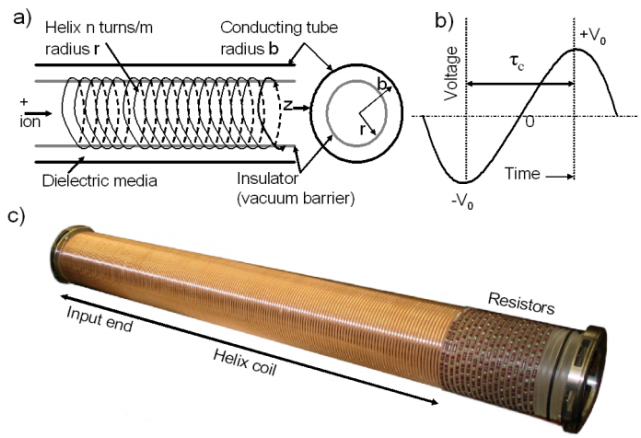

Figure 4: a) A schematic of the helical pulse line structure, b) schematic of a drive voltage waveform applied at the helix input; and c) mechanically constructed helix for the PLIA experiments.

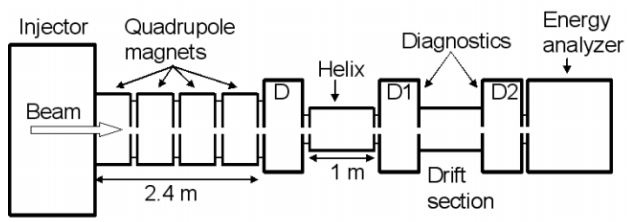

Figure 5: Experimental configuration of the PLIA with a K^+ beam injector, transported by four pulsed quadrupole magnets, 1 m long helix section, diagnostics, and an electrostatic energy analyzer.

Energy Gain

A voltage pulser is applied to the input end of the PLIA. Figure 6 shows the bipolar helix voltage waveform used for these initial tests of PLIA beam dynamics. For these experiments, the voltage swing is limited to 33 kV, in order to maintain shot-to-shot reproducibility. This corresponds to an average ion acceleration gradient of ~150kV/m. Even at that voltage, flashover is observed

(light emission) on the interior of the helix beam tube, but the waveforms at the exit are reproducible.

The helix voltage pulse is applied to the plateau portion of the beam, between 10 and 15 μs after the beam head, where the energy is nearly constant at the PLIA entrance. The initially flat energy profile then exhibits pronounced peaks and valleys. As expected, the portions of the beam riding on the positive slopes of the waveform are accelerated while the beam particles riding on the negative slopes are decelerated. Indeed, the frequency in the longitudinal phase space coincides with that of the helix voltage waveform, and the five peaks and valleys of varying magnitudes in Fig. 7(a) can be correlated with the positive and negative slopes of the voltage waveform. In these experiments, the beam energy ranged between above 270 and 500 keV along the pulse, corresponding to an energy change between -80 keV and +150 keV. Note that the helix voltage has a maximum range of -21 kV to +12 kV (Fig.6). The result of a WARP particle-in-cell simulation is shown in Fig. 7(b), using an axisymmetric model with electrostatic beam self fields.

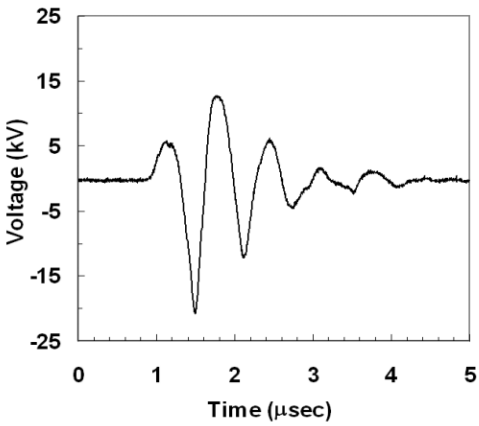

Figure 6: Voltage waveform measured at the exit of the helix. The voltage and time interval associated with the first full peak-to-peak swing are ~33 kV and ~300 ns, respectively.

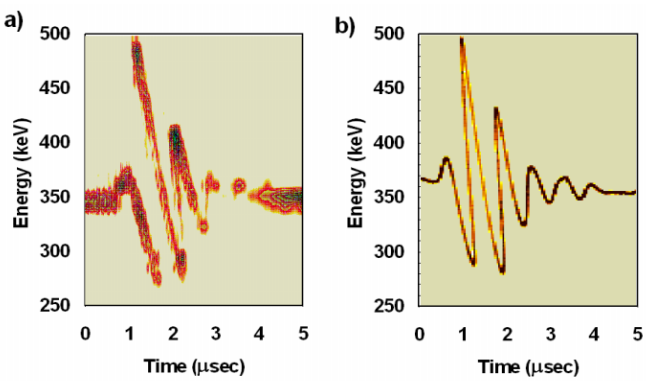

Figure 7: a) Time-energy phase space of 350 keV beam after passing through the energized PLIA; and b) WARP3D simulation for similar conditions.

Also, multiple peaks are observed in the current profile [20], coinciding with the upward swings of the helix voltage pulse. Two of the peaks of beam current are double peaks, with sharp spikes at the start and end of the peak; this structure is due to particle overtaking (wave breaking) in the (z,v_z) phase space. The WARP simulation yields similar structures. We observe very similar structures in previous neutralized drift compression experiments [15]. The structure and location of the current peaks from particle overtaking are very sensitive to the details of the helix waveform propagation and diagnostics location.

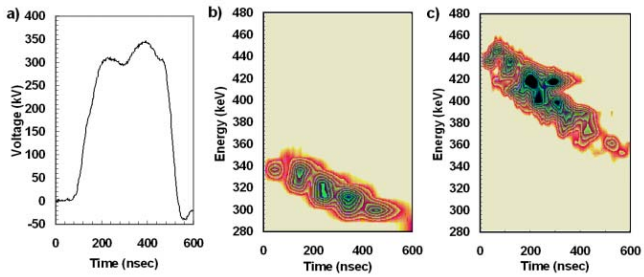

Figure 8: Short-beam experiment on PLIA: (a) Marx voltage waveform; (b) beam time-energy phase space without helix power; and (c) phase space with helix powered.

As an example of how the PLIA can accelerate whole bunches, a short pulse was accelerated as shown in Fig. 8. To perform this experiment, the Marx voltage pulse was shortened to 350 ns (FWHM) [see Fig. 8(a)], which is comparable to the beam transit time through the injector diode. The beam dynamics in the diode now differs substantially from the steady-state Child-Langmuir flow characteristic of the long pulse. These transient effects lead to a short pulse with a large energy tilt from head to tail [Fig. 8(b)]. When the helix voltage pulse is applied by synchronizing the short pulse to the rising portion of the helix voltage waveform, the entire beam bunch is accelerated. The resulting longitudinal phase space is shown in Fig. 8(c). Note that the energy tilt of the beam bunch is also increased, illustrating the potential flexibility in manipulating the longitudinal phase space by varying the input voltage waveform and beam timing. This feature is of great value in controlling the longitudinal space-charge debunching effects of an intense short pulse, as well as in providing the necessary velocity tilt for neutralized drift compression.

Mitigation of Flashover and Achieving Higher Energy Gain

The helix configuration with a simple long straight-wall glass insulator used in these experiments exhibited surface flashover of the vacuum insulator at a few kV/cm. In attempts to mitigate this limitation, the inner surface of the helix was coated with chromium oxide, and better grounding of the inner diameter of the glass tube at the ends were explored to avoid possible

surface charging phenomena. However, maintaining the coating uniformity and the desired resistivity proved difficult and these efforts did not lead to an improved performance of the helix. Experiments with the helix inside a solenoid producing 200-300 G also did not significantly alter the flashover threshold. Future experiments will test several new configurations and ideas:

(1) An epoxy helix design where the helix windings protrude from the epoxy into the vacuum has been fabricated to see if the grading of the vacuum interface with this geometry improves the performance.

(2) A helix with the original long straight-wall glass insulator has been modified by adding many shorted rings at the outer diameter to attenuate the pulsed magnetic field at the vacuum surface of the insulator. This experiment will test the hypothesis that the pulsed magnetic field produced by the traveling wave could be contributing to the surface flashover mechanism.

(3) Recently, numerical modeling has suggested that a multipactor-like phenomenon could be occurring at the vacuum surface of the glass [21,27]. High voltage tests are planned to investigate the dependence of the breakdown on the voltage waveform to see if the bipolar waveform enhances this mechanism.

(4) A more expensive backup insulator design is a conventional ceramic column with grading rings and a commercially available resistive coating on the vacuum surface. Depending on the results from the tests described above the rings may be open or closed, although for ion beam experiments with pulsed solenoids for ion beam transport [24] we may need open rings to prevent attenuation of the focusing magnetic field.

SUMMARY

Significant physics results on beam compression have been demonstrated. Simultaneous transverse and longitudinal compression experiments are in progress. The predicted energy amplification and beam bunching in the PLIA has been experimentally observed. The vacuum flashover, which presently limits the acceleration gradient to $\leq$150 kV/m is being investigated. When solved, the PLIA concept has the potential to achieve high acceleration gradients at a modest cost.

ACKNOWLEDGEMENT

This research was performed under the auspices of the U.S. Department of Energy by the University of California Lawrence Livermore and Lawrence Berkeley National Laboratories and the Princeton Plasma Physics Laboratory, under Contract Nos. W-7405-Eng-48, DE-AC02-05CH11231, and DE-AC02-76CH03073.

REFERENCES

[1] P. Renaudin et al., Phys. Rev. Lett. **91**,075002 (2003).
[2] J. J. Barnard et al, *Proc. of the 2005 Particle Accelerator Conf.*, edited by C. Horak, (IEEE, 2005), p. 2568.
[3] W. M. Sharp et al., Nucl. Instrum. Meth. Phys. Res. A **544**, 398 (2005).
[4] S. S. Yu et al., *Proc. of the 2003 Particle Accelerator Conf.*, edited by J.Chew, (IEEE, 2003), p. 98.
[5] E. Henestroza, et al., Phys. Rev. ST Accel. Beams **7**, 083501 (2004).
[6] P. K. Roy et al., Phys. of Plasmas **11**, 2890 (2004).
[7] B. G. Logan et al., Nucl. Fusion **45**, 131 (2005).
[8] C. Thoma et al., Phys. of Plasmas **12**, 043102 (2005).
[9] P. K. Roy et al., Nucl. Instrum. Meth. Phy. Res. A **544**, 225 (2005).
[10] D. D.-M. Ho et al., Particle Accel. **35**, 15 (1991).
[11] T. Kikuchi et al., Phys. of Plasmas **9**, 3476 (2002).
[12] H. Qin et al., Phys. Rev. ST Accel. Beams **7**, 104201 (2004).
[13] R. C. Davidson et al., Phys. Rev. ST Accel. Beams **8**, 064201 (2005).
[14] W. M. Fawley et al., Phys. Plasmas **4**, 880 (1997).
[15] P. K. Roy et al., Phys. Rev. Lett. **95**,234801 (2005).
[16] R. J. Briggs et al., in *Proc. of the 2005 Particle Accelerator Conf.*, edited by C. Horak, (IEEE, 2005), p.440.
[17] R. J. Briggs et al., Phys. Rev. ST Accel. Beams **9**, 060401 (2006).
[18] A. Friedman et al., in *Proc. of the 2005 Particle Accelerator Conf.*, (IEEE, 2005), p.339.
[19] E. Henestroza et al., in *Proc. of the 2005 Particle Accelerator Conf.*, edited by C. Horak, (IEEE, 2005), p.2032.
[20] P. K. Roy et al., Phys. Rev. ST Accel. Beams **9**, 070402 (2006).
[21] J. E. Coleman et al., to be published in Proce. of the 16th Heavy Ion Fusion symposium (2006) .
[22] A. B. Sefkow, et. al., Phys. Rev. ST - Accel. Beams **9**, 052801 (2006).
[23] D. R. Welch et al., Nucl. Instrum. Methods Phys. Res., Sect. A **544**, 236 (2005).
[24] P. A. Seidl et al., to be published in Proce. of the 16th Heavy Ion Fusion symposium (2006).
[25] A. Sefkow et al., to be published in Proce. of the 16th Heavy Ion Fusion symposium (2006).
[26] P. Efthimion et al., to be published in Proce. of the 16th Heavy Ion Fusion symposium (2006).
[27] A. Friedman et al., to be published in Proce. of the 16th Heavy Ion Fusion symposium (2006).